

Scalar lumps with one and two horizons

George Lavrelashvili

A.Razmadze Mathematical Institute
at I.Javakhishvili Tbilisi State University

RAFP, Sept 28, 2022

Plan

- Motivation
- Introduction
- The setup
- Analytical & Numerical results
- Concluding remarks

(Personal) Motivation

Black holes, oscillating instantons and the Hawking-Moss transition

Ruth Gregory,^{a,b,c} Ian G. Moss^d and Naritaka Oshita^c

^a*Institute for Particle Physics Phenomenology, Department of Physics, Durham University, South Road, Durham, DH1 3LE, U.K.*

^b*Department of Mathematical Sciences, Durham University, South Road, Durham, DH1 3LE, U.K.*

^c*Perimeter Institute, 31 Caroline Street North, Waterloo, ON, N2L 2Y5, Canada*

^d*School of Mathematics, Statistics and Physics, Newcastle University, Newcastle Upon Tyne, NE1 7RU, U.K.*

E-mail: r.a.w.gregory@durham.ac.uk, ian.moss@newcastle.ac.uk, noshita@pitp.ca

ABSTRACT: Static oscillating bounces in Schwarzschild de Sitter spacetime are investigated. The oscillating bounce with many oscillations gives a super-thick bubble wall, for which the total vacuum energy increases while the mass of the black hole decreases due to the conservation of Arnowitt-Deser-Misner (ADM) mass. We show that the transition rate of such an “up-tunneling” consuming the seed black hole is higher than that of the Hawking-Moss transition. The correspondence of analyses in the static and global coordinates in the Euclidean de Sitter space is also investigated.

T.Torii, K.Maeda and M.Narita,
“Can the cosmological constant support a scalar field?,”
Phys. Rev. D 59 (1999), 104002

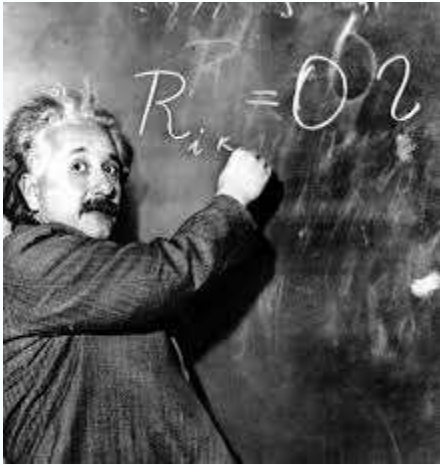
T.Torii, K.Maeda and M.Narita,
“No scalar hair conjecture in asymptotic de Sitter space-time,”
Phys. Rev. D59 (1999), 064027, arXiv:gr-qc/9809036 [gr-qc].

M.S.Volkov, N.Straumann, G.Lavrelashvili, M.Heusler and O.Brodbeck,
“Cosmological analogs of the Bartnik-McKinnon solutions,”
Phys. Rev. D54 (1996), 7243, arXiv:hep-th/9605089 [hep-th].

G.Lavrelashvili, J.L.Lehners and M.Schneider, “Scalar lumps with a horizon,”
Phys. Rev. D104 (2021) 044007, arXiv:2104.13403 [hep-th].

G.Lavrelashvili and J.L.Lehners, “Scalar lumps with two horizons,”
Phys. Rev. D10 (2022) 024051, arXiv:2109.04180 [gr-qc].

Introduction: solitons and black holes

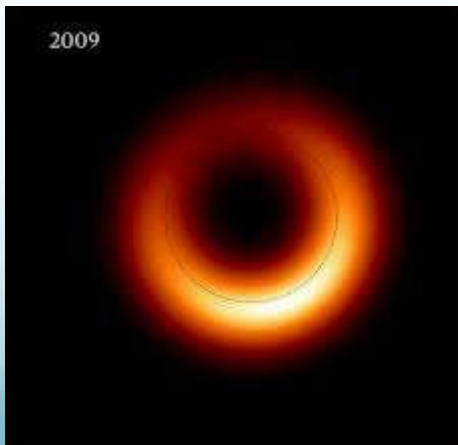


- $R_{\mu\nu} - \frac{1}{2} g_{\mu\nu} R = \frac{8\pi G}{c^4} T_{\mu\nu} + \Lambda g_{\mu\nu}$
- Matter field equations = 0

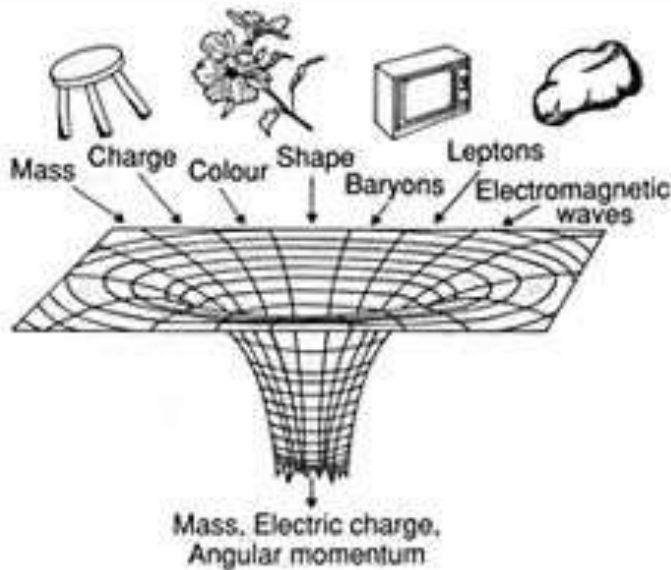
- $ds^2 = -A dt^2 + \frac{dr^2}{B} + r^2 d\Omega^2$

- $A(r), B(r)$ - metric

- $\varphi(r), W(r), \dots$ - matter



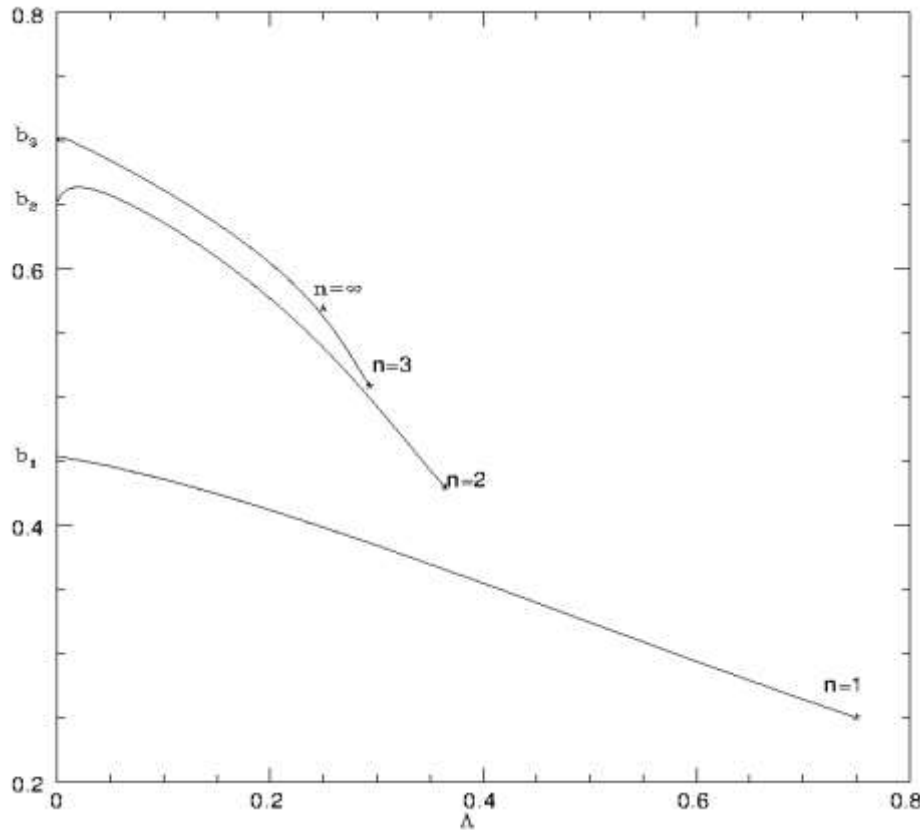
Colored black holes :



- **G.Lavrelashvili**, D.Maison, "Regular and black hole solutions of Einstein Yang-Mills Dilaton theory", Nucl.Phys. B410 (1993) 407-422.
- **G.Lavrelashvili**, D.Maison, "Static spherically symmetric solutions of a Yang-Mills field coupled to a dilaton", Phys.Lett. B295 (1992) 67-72.
- **G.Lavrelashvili**, "Fermions in the background of dilatonic sphalerons", Mod.Phys.Lett. A9 (1994) 3731-3740.



Non-Abelian solitons and black holes in (anti) de Sitter space:



n	$\Lambda_{crit}(n)$	$\Lambda_{\infty}(n)$	$\Lambda_{*}(n)$
1	0.330	0.334	0.75
2	0.239	0.250	0.364
3	0.237	0.247	0.293

- M.S.Volkov, N.Straumann, **G.Lavrelashvili**, M.Heusler, O.Brodbeck, "Cosmological analogs of the Bartnik-McKinnon solutions", Phys.Rev. D54 (1996) 7243-7251.
- P.Breitenlohner, **G.Lavrelashvili**, D.Maison, "Non Abelian gravitating solitons with negative cosmological constant", Class.Quant.Grav. 21 (2004) 1667-1684.

The setup

Let us consider a self-interacting scalar field theory minimally coupled to gravity, with action

$$S = \int d^4x \sqrt{-g} \left[\frac{1}{2\kappa} \mathcal{R} - \frac{1}{2} g^{\mu\nu} \partial_\mu \varphi \partial_\nu \varphi - V(\varphi) \right], \quad (1)$$

where $\kappa = 8\pi G$.

In what follows, we will be interested in static, spherically symmetric fields and parametrize the metric as

$$ds^2 = -f(r) e^{2\delta(r)} dt^2 + \frac{dr^2}{f(r)} + R^2(r) d\Omega_2^2. \quad (4)$$

Schwarzschild gauge

As long as $R'(r) \neq 0$, we can choose Schwarzschild gauge $R(r) \equiv r$.

$$\varphi'' = -\left(\frac{2}{r} + \frac{f'}{f} + \delta'\right)\varphi' + \frac{1}{f} \frac{\partial V}{\partial \varphi}, \quad (6)$$

$$rf' = 1 - f - \kappa r^2 \left(\frac{1}{2}f\varphi'^2 + V\right), \quad (7)$$

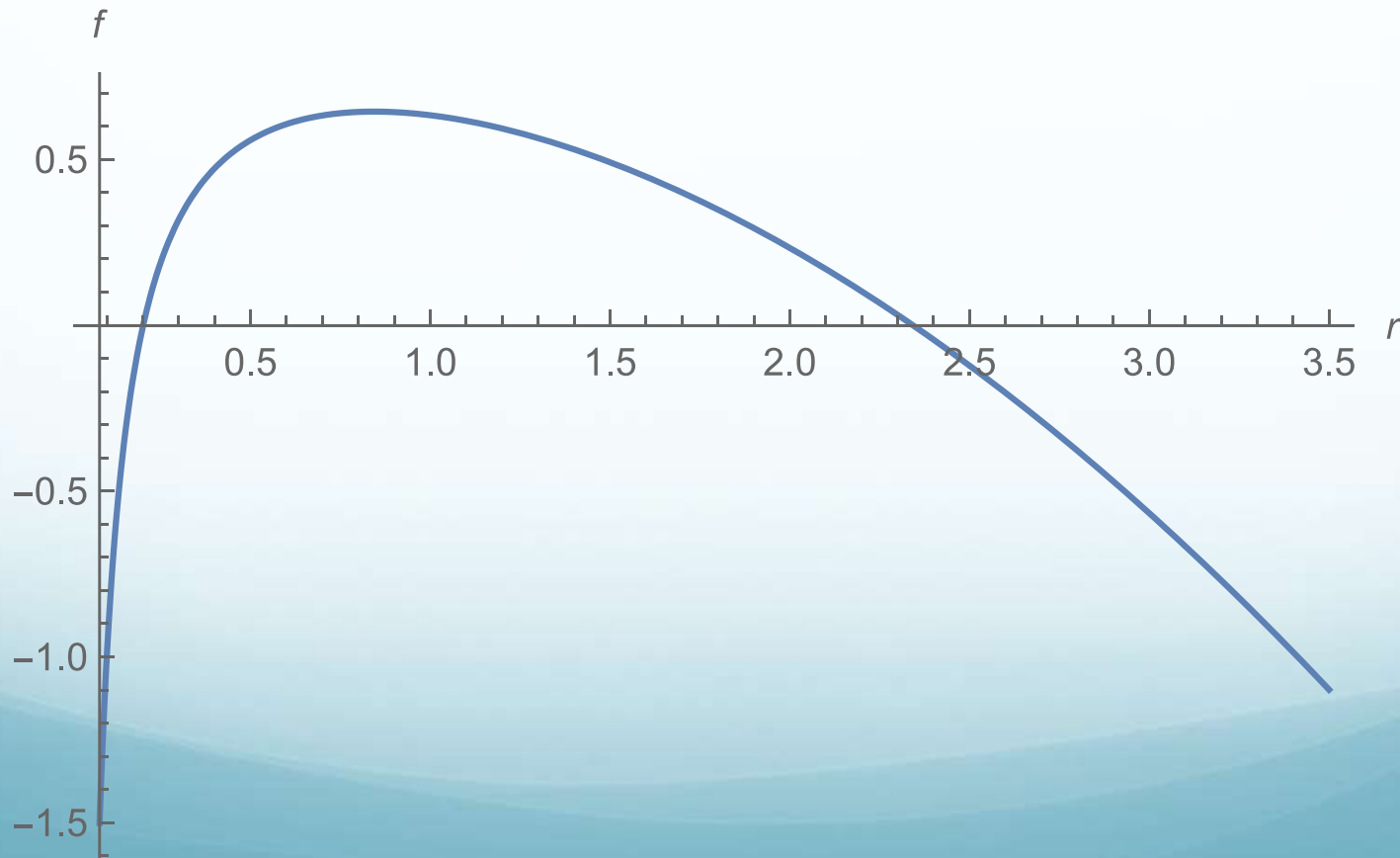
$$\delta' = \frac{\kappa}{2}r\varphi'^2. \quad (8)$$

Schwarzschild-de Sitter solution

$$f_0(r) = 1 - \frac{2\kappa M_0}{r} - \frac{\kappa V(\varphi_m)}{3} r^2$$

Schwarzschild-de Sitter space-time

$$f(r) = 1 - \frac{2M}{r} - \frac{\Lambda}{3}r^2, R(r) = r, \phi = 0$$



General gauge

If at some point $R'(r) = 0$, the Schwarzschild gauge becomes inappropriate. In such a case, we may set $\delta \equiv 0$ while leaving $R(r)$ general, and we call this choice “general” gauge. Varying the reduced action (5) with respect to φ , R , and f , we obtain the corresponding field equations

$$\varphi'' = -\left(2\frac{R'}{R} + \frac{f'}{f}\right)\varphi' + \frac{1}{f}\frac{\partial V}{\partial\varphi}, \quad (18)$$

$$f'' = -2\frac{R'}{R}f' - 2\kappa V, \quad (19)$$

$$R'' = -\frac{\kappa}{2}R\varphi'^2, \quad (20)$$

while variation with respect to δ , prior to setting it to zero, gives the constraint equation

$$f\frac{R'^2}{R^2} + f'\frac{R'}{R} = \frac{1}{R^2} + \kappa\left(\frac{1}{2}f\varphi'^2 - V\right). \quad (21)$$

Regular Singular Point of ordinary differential equation

Definition of Regular Singular Points

Let

$$P(x)y'' + Q(x)y' + R(x)y = 0$$

be a linear second order differential equation. Then x_0 is called a *regular singular* point if

$$\lim_{x \rightarrow x_0} (x - x_0) \frac{Q(x)}{P(x)}$$

and

$$\lim_{x \rightarrow x_0} (x - x_0)^2 \frac{R(x)}{P(x)}$$

are both finite.

Close to regular origin
we have 1 free parameter:

$$\varphi(r) = \varphi_0 + \frac{V'(\varphi_0)}{6} r^2 + V'(\varphi_0) \left(\frac{\kappa V(\varphi_0)}{36} + \frac{V''(\varphi_0)}{120} \right) r^4 + O(r^6), \quad (9)$$

$$f(r) = 1 - \frac{\kappa V(\varphi_0)}{3} r^2 - \frac{\kappa V'(\varphi_0)^2}{60} r^4 + O(r^6), \quad (10)$$

$$R(r) = r - \frac{\kappa V'(\varphi_0)^2}{360} r^5 + O(r^7), \quad (11)$$

where φ_0 is a free parameter.

Close to horizon, $f(r_h)=0$,
we find 4 free parameters:

$$\varphi(\rho) = \varphi_h + \frac{V'(\varphi_h)}{f'_h} \rho + \frac{V'(\varphi_h)[2\kappa V(\varphi_h) + V''(\varphi_h)]}{4f_h'^2} \rho^2 + O(\rho^3), \quad (23)$$

$$f(\rho) = f'_h \rho - \frac{1}{R_h^2} \rho^2 + O(\rho^3), \quad (24)$$

$$R(\rho) = R_h + \frac{1 - \kappa R_h^2 V(\varphi_h)}{f'_h R_h} \rho - \frac{\kappa R_h V'(\varphi_h)^2}{4f_h'^2} \rho^2 + O(\rho^3), \quad (25)$$

where $\rho \equiv r - r_h$ and r_h , f'_h , φ_h , and R_h are free parameters.

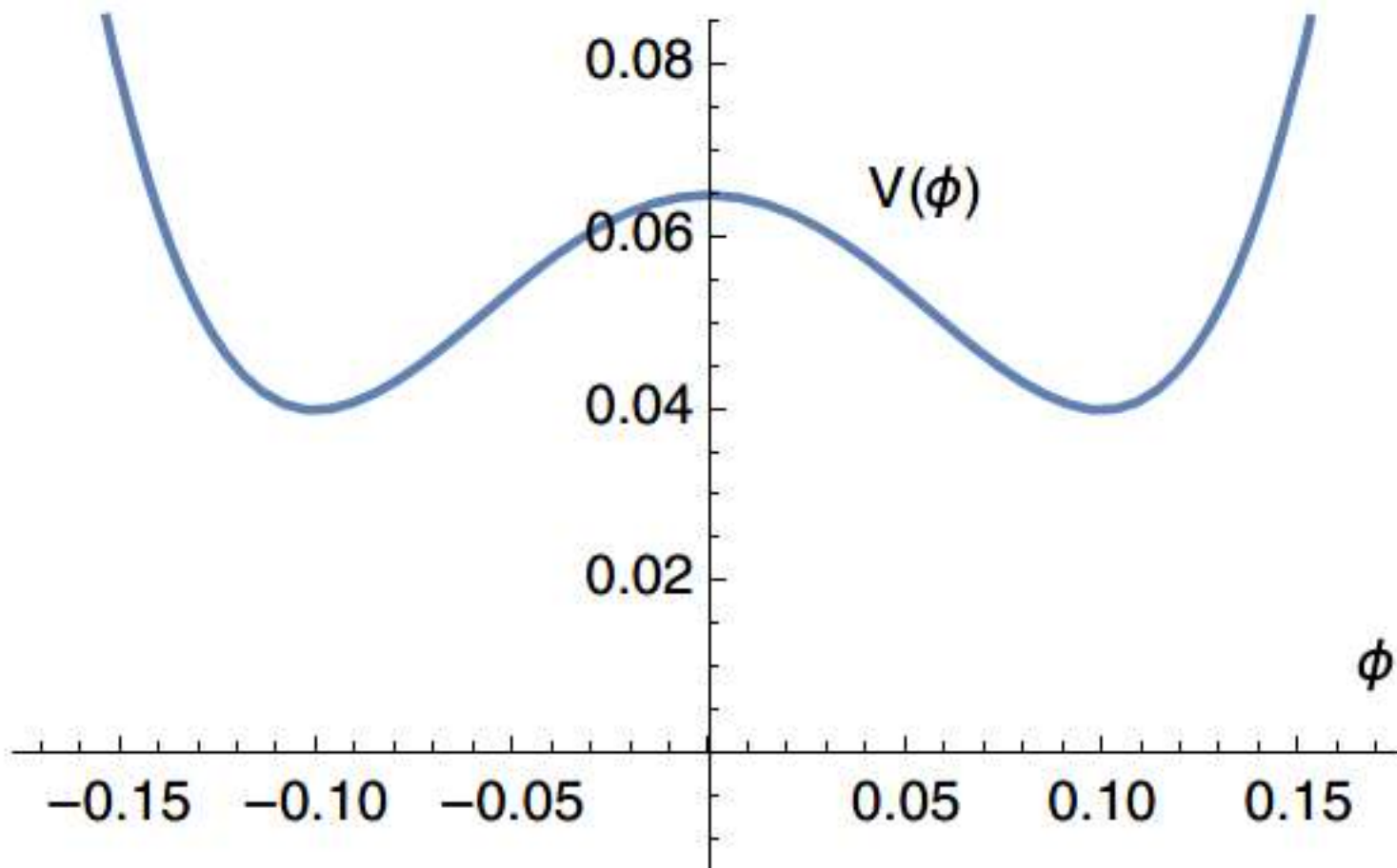
The scalar potential that we will consider is of double-well form,

$$V(\varphi) = \frac{\Lambda}{\kappa} + \frac{\lambda}{4}(\varphi^2 - v^2)^2, \quad (26)$$

where we have also included a cosmological constant Λ . This potential contains a local maximum at $\varphi = 0$, of magnitude $V(0) = \frac{\Lambda}{\kappa} + \frac{\lambda}{4}v^4$, and two minima at $\varphi = \pm v$. In what follows, we will use $G = 1$ units (implying $\kappa = 8\pi$). Furthermore, as shown in Ref. [2], the fields may be redefined so as to effectively set $\Lambda = 1$. This implies that we do not have to consider different values for the cosmological constant in searching for solutions, and specifying only the parameters λ and v of the potential is sufficient.

განვიხილოთ კონკრეტული პოტენციალი

$$V(\varphi) = \frac{\Lambda}{\kappa} + \frac{\lambda}{4} (\varphi^2 - v^2)^2$$



Parameter count, numerical strategy

Our numerical strategy is as follows. In general gauge, we have three functions, $f(r)$, $R(r)$, and $\phi(r)$ satisfying second-order equations, which implies that one needs to specify six parameters to fix a solution. The constraint equation (21) reduces the number of free parameters by 1, leaving one with only five free parameters required for specifying a solution. As shown above in Eqs. (23), (24), (25), close to a horizon, we have four free parameters. At the first and second horizons, we will, respectively, call these parameters $r_{1,2}$, $f'_{1,2}$, $\varphi_{1,2}$, and $R_{1,2}$; i.e., we have eight parameters in total.

With our metric ansatz, there actually remains some residual gauge freedom; note that equations of motions are translationally invariant with respect to a shift of the variable r ,

$$r \rightarrow r + \Delta, \quad (27)$$

and scale invariant with respect to the transformations

$$r \rightarrow \alpha r, \quad f \rightarrow \alpha^2 f, \quad (28)$$

with arbitrary parameters Δ and α . These transformations allow us to fix the coordinate location of the first horizon to be at the origin, $r_1 = 0$, and they also allow us to fix the derivative of f at the location of the first horizon—we will set $f'_1 = 1$. We are left with six parameters. Since a solution is specified by fixing five parameters, we are left with one parameter, which we can choose freely. We will choose this free parameter to be the first horizon size R_1 . This freedom is equivalent to specifying the mass M_0 in the SdS solution

Counting the number of parameters of the solutions

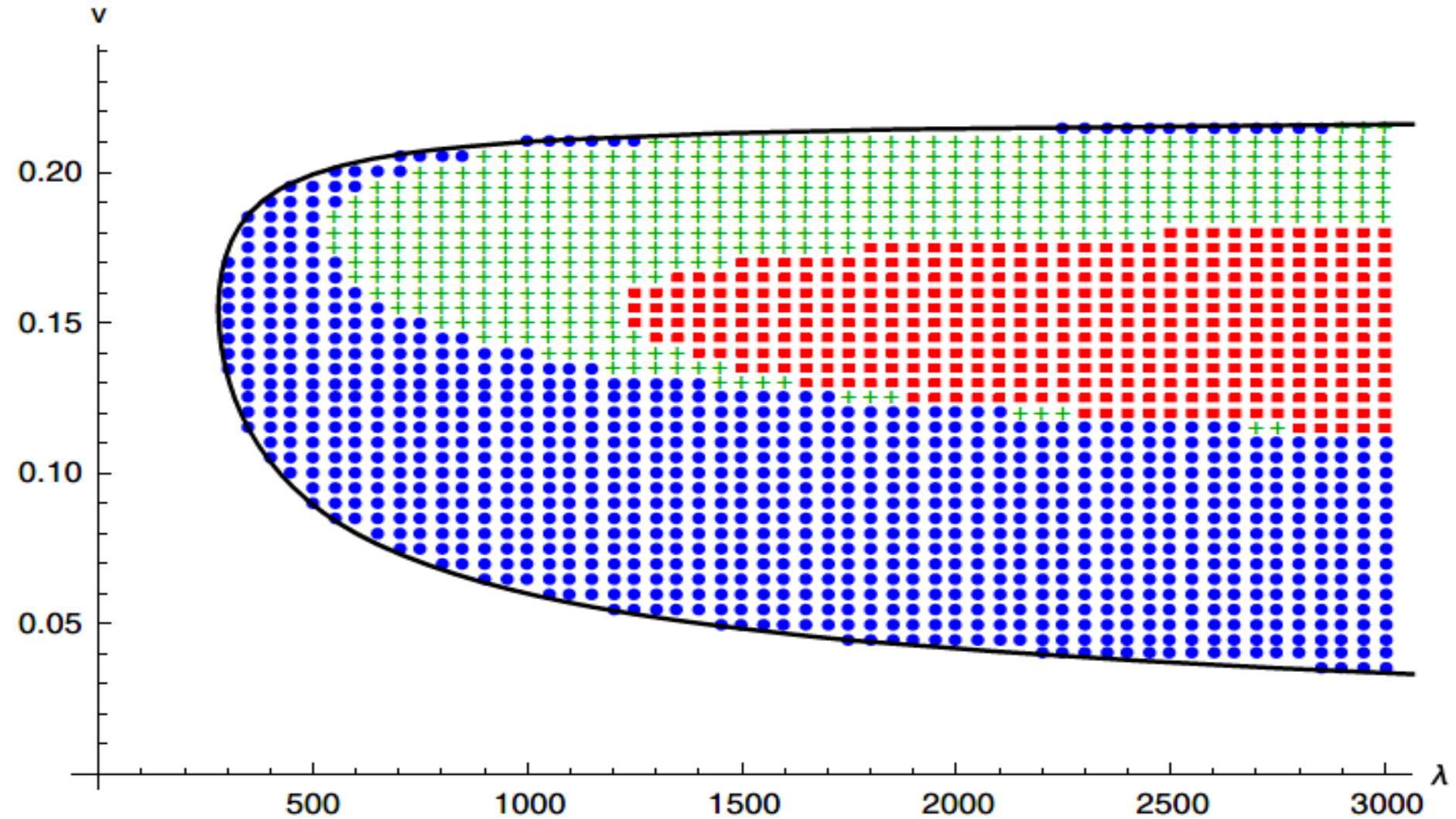
- 3 functions satisfy the second order differential equations - 1 constraint = $6 - 1 = 5$ parameters are needed to specify solution
- Regular origin: 1 parameter at the origin + 4 parameters at the horizon = 5 free parameters
- Two horizon case: 4 free parameters at the first horizon + 4 free parameters at the second horizon = $8 - 2$ symmetry = 6, i.e. one parameter is free.

$$r \rightarrow r + \Delta,$$

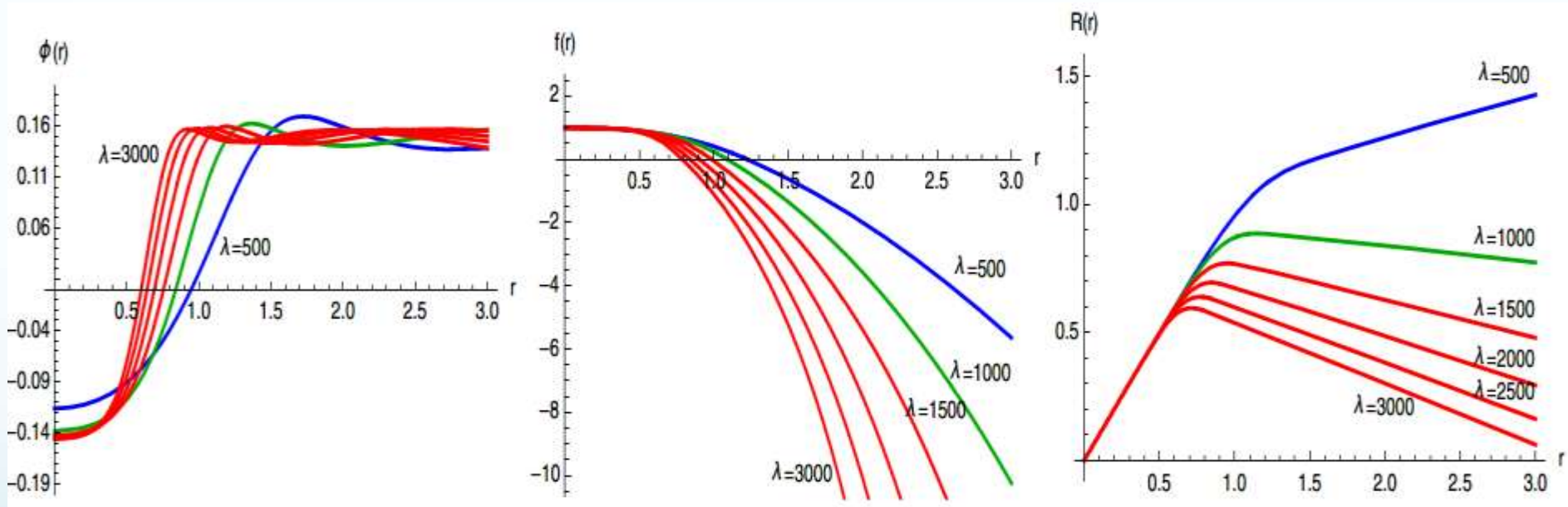
$$r \rightarrow \alpha r, \quad f \rightarrow \alpha^2 f$$

In practical calculations, we thus first fix the first horizon size R_1 . We then solve the field equations starting from some small ϵ away (typically of order 10^{-5}) from the two horizons, with initial conditions given by the expansions in Eqs. (23), (24), and (25), in the direction of positive f . As explained above, at the first horizon, $r_1 = 0$, $f'_1 = 1$, and thus we only have a single free parameter there, namely, φ_1 . From both horizons, we solve the equations of motion until $f(r)$ reaches a maximum. At this location, we match the two half-solutions together. This has two consequences: the first is that f' is automatically continuous, and the second is that the coordinate location r_2 of the second horizon is implied. We then use a Newtonian algorithm to optimize all of the free parameters, until the fields and their derivatives are continuous at the matching location with sufficient precision.

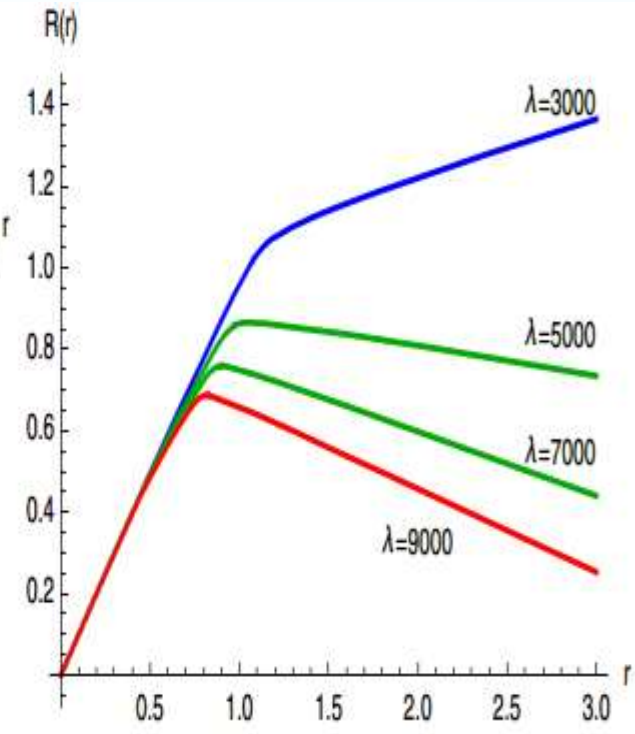
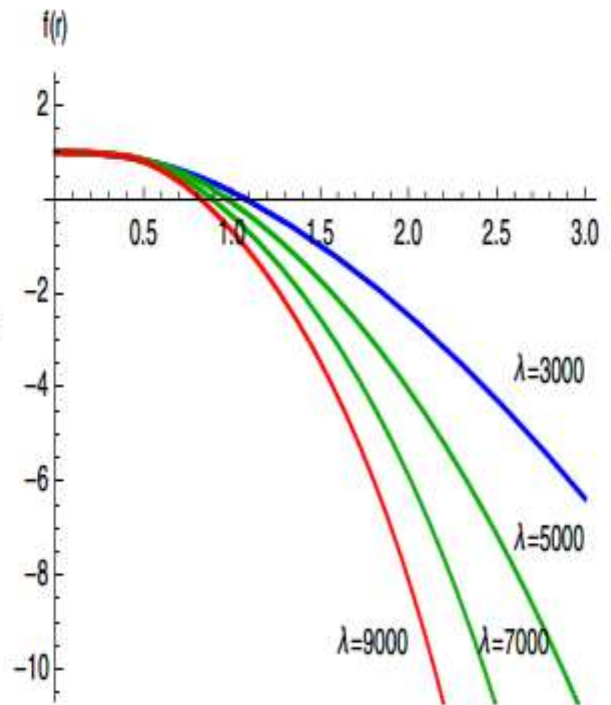
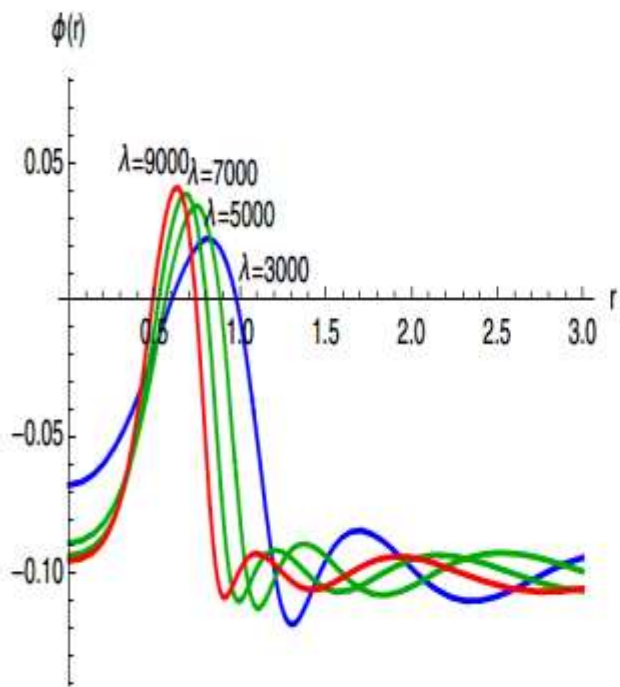
Three classes of solutions: parameter space



Three classes of solutions: : profiles of the functions for $n=1$



Three classes of solutions: : profiles of the functions for $n=2$



Solutions with two horizons

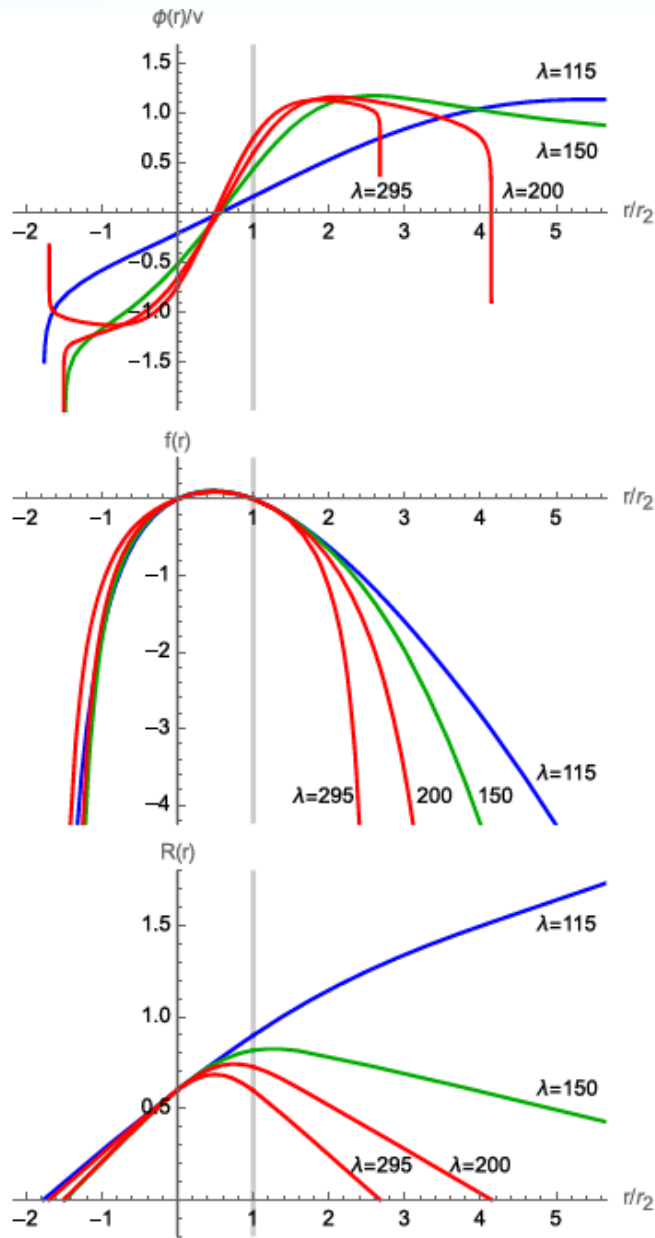
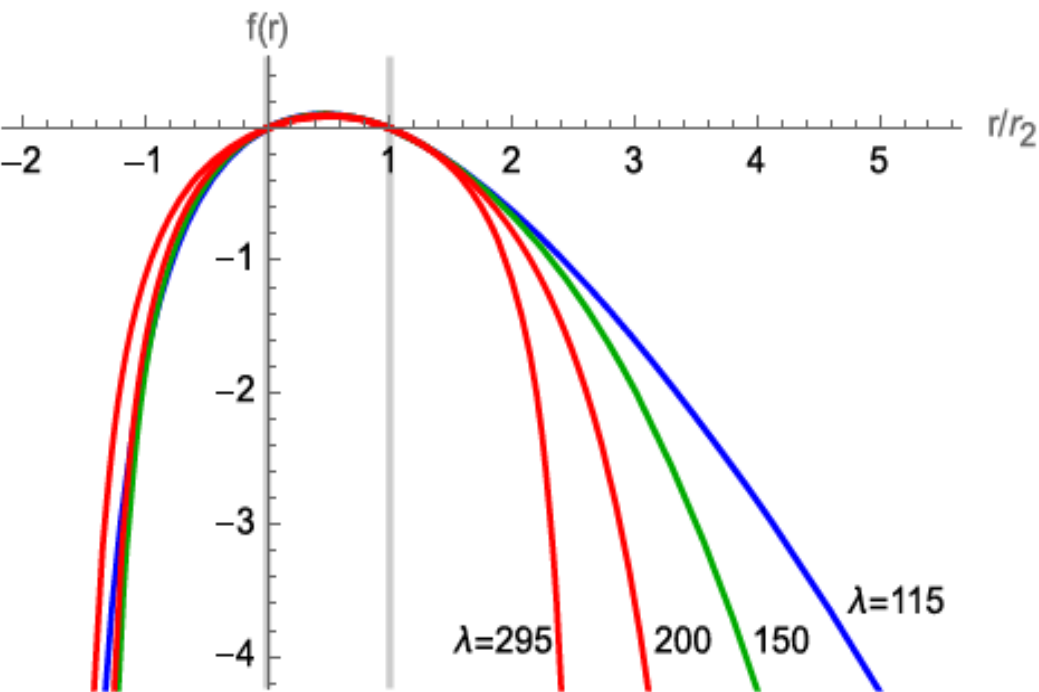
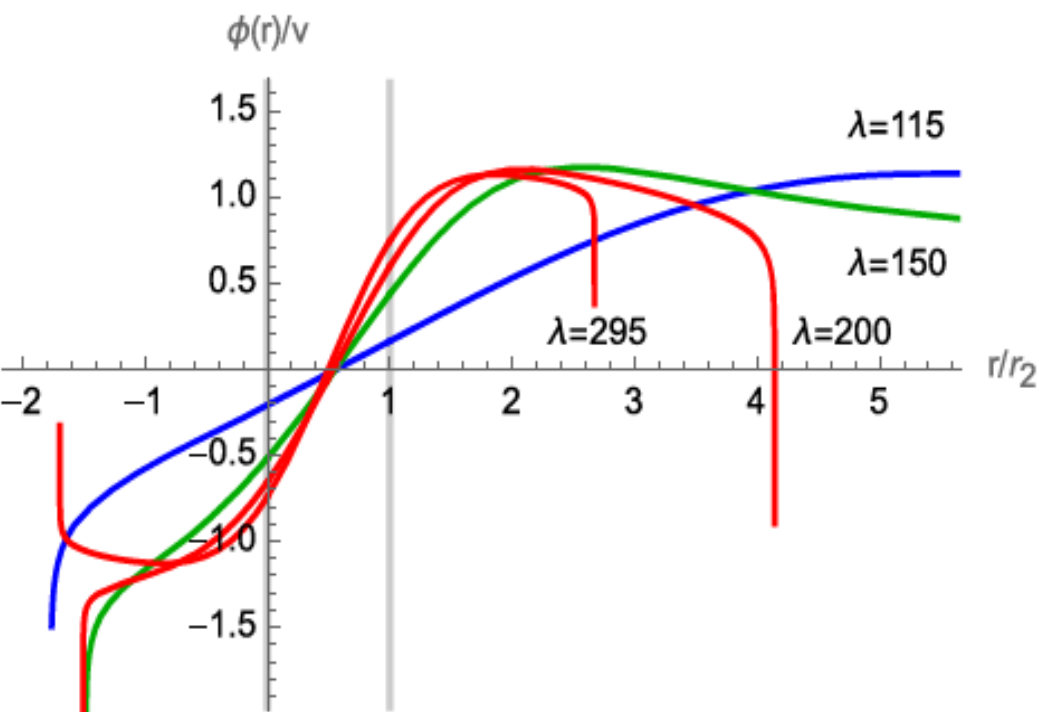


FIG. 1. Examples of solutions with the potential “width” fixed at $v = 0.18$ for various coupling constants λ . For all of these solutions, the first horizon size is set at $R_1 = 0.6$ and resides at $r = 0$. The location of the horizons is indicated by the thick vertical gray lines (one being at the origin $r = 0$). The scalar field is rescaled such that the minima of the potential reside at ± 1 . Also, these solutions have been plotted as functions of $r/(r_2 - r_1) = r/r_2$ in order to facilitate a comparison; the second horizon then always resides at $r/r_2 = 1$. See the main text for a full description.

TABLE I. Optimized horizon values for the solutions in Fig. 1, given here to three significant digits.

λ	φ_1	φ_2	f'_2	R_2
115	-0.0376	0.0291	0.765	0.898
150	-0.0935	0.0784	0.828	0.817
200	-0.118	0.107	0.900	0.726
295	-0.134	0.134	1.000	0.598



- Examples of different classes of solutions:
- Blue (monotonic R)
- Green (R has maximum after second horizon)
- Red (R has maximum between horizons)

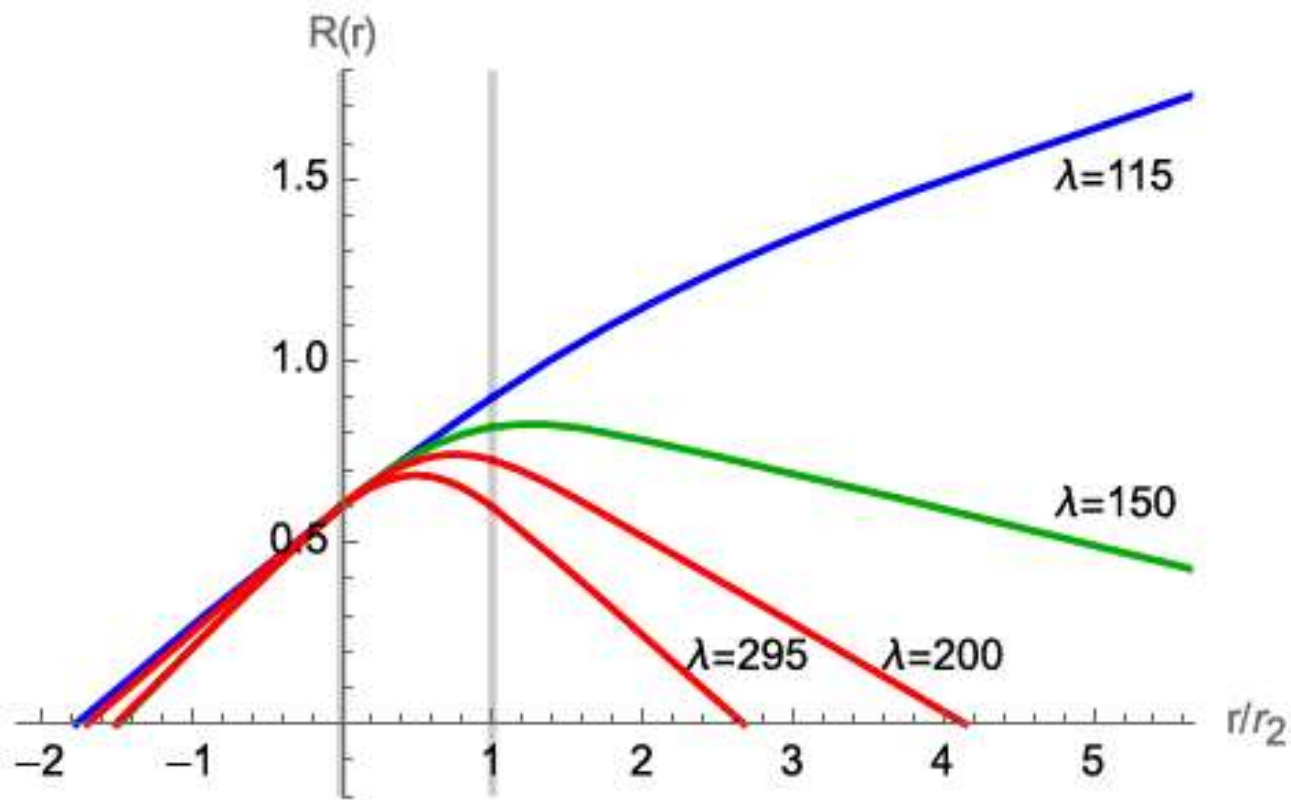


FIG. 1. Examples of solutions with the potential “width” fixed at $v = 0.18$ for various coupling constants λ . For all of these solutions, the first horizon size is set at $R_1 = 0.6$ and resides at $r = 0$. The location of the horizons is indicated by the thick vertical gray lines (one being at the origin $r = 0$). The scalar field is rescaled such that the minima of the potential reside at ± 1 . Also, these solutions have been plotted as functions of $r/(r_2 - r_1) = r/r_2$ in order to facilitate a comparison; the second horizon then always resides at $r/r_2 = 1$. See the main text for a full description.

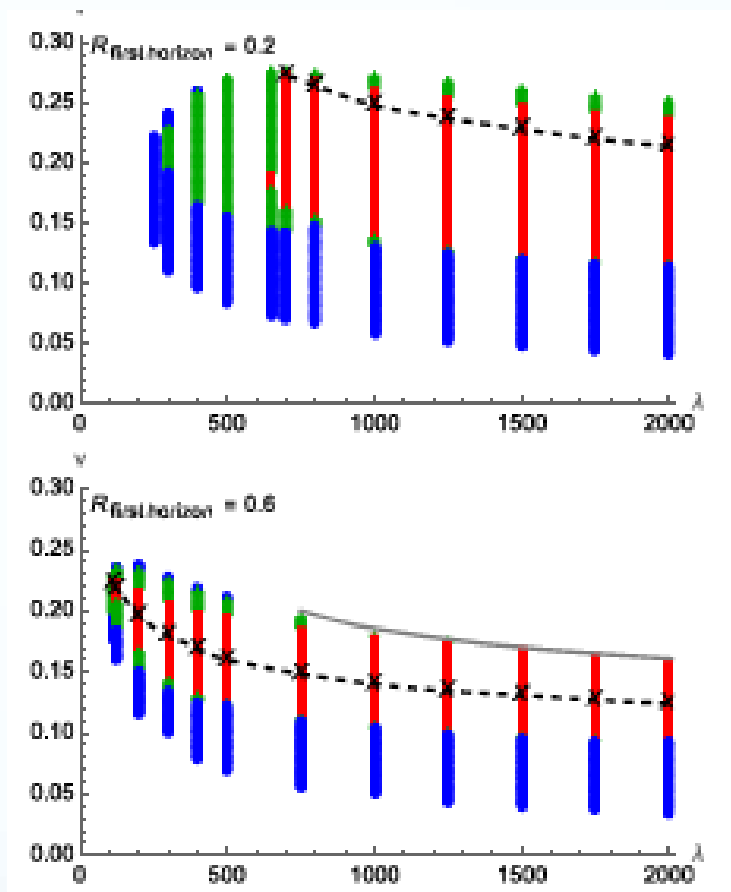
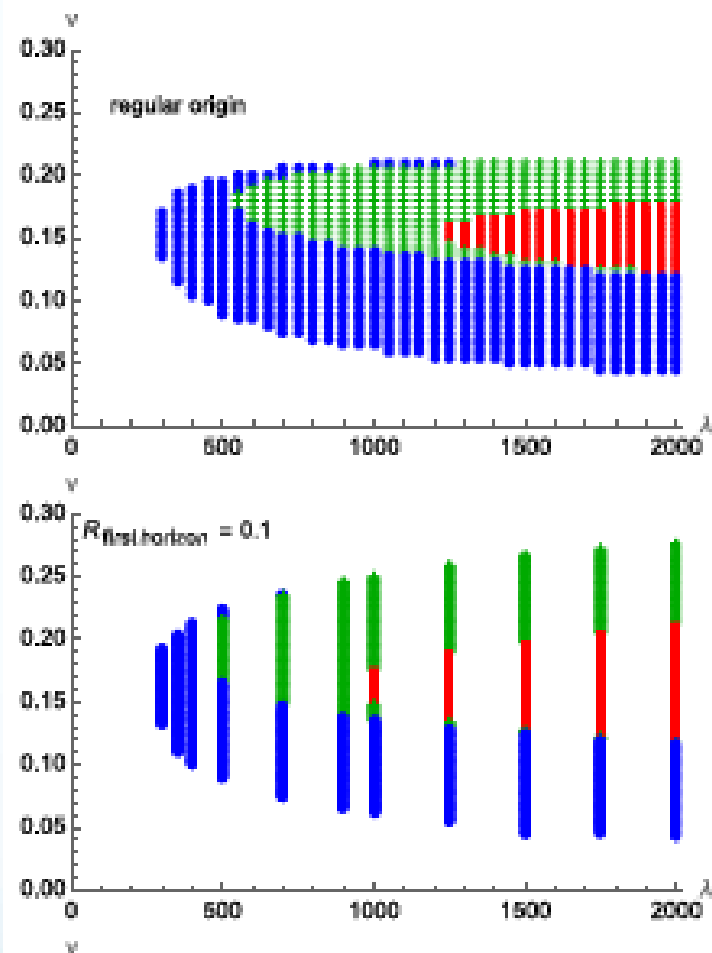


FIG. 3. Overview plots for different sizes R_1 of the first horizon, as a function of the parameters λ , v in the potential. We also included a reference plot at the top of the existence of solutions with a regular origin and a single horizon. Blue dots indicate the existence of solutions with monotonic $R(r)$, green crosses indicate solutions in which $R(r)$ turns around outside of a horizon, and red squares indicate double-black-hole solutions in which $R(r)$ turns around in between the two horizons. A full description is given in the main text.

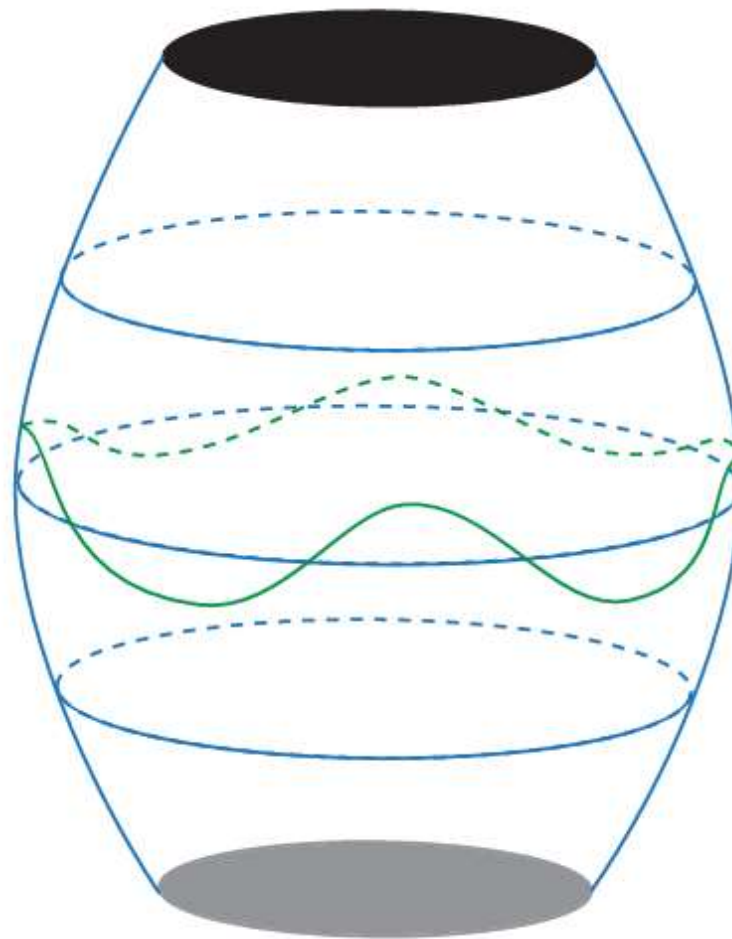


FIG. 10. A drawing of the solutions with nonmonotonic $R(r)$. Depicted here are only the r direction and a transverse circle instead of transverse spheres. The spacetime is capped off by two black holes, one on each pole. In green, we show a particle undergoing accelerated motion near the equator, which itself represents an unstable orbit. If the particle travels too close to either black hole, it will inexorably be pulled in. The vacuum energy changes across the spacetime: it interpolates between the two sides of the scalar potential barrier as one traverses from one black hole to the other.

Conclusions :

- We studied self-interacting scalar field theory coupled to gravity and found scalar lumps with regular origin surrounded by a horizon and scalar lumps with two horizons.
- New classes of solutions with non-monotonic function $R(r)$ are found
- In particular we found static, spherically symmetric solutions with two black holes.
- It is interesting to search globally regular solutions of this system, analogues to the ones found in the EYMA theory.

Thanks for attention!



Supported by

**Shota Rustaveli National Science
Foundation of Georgia Grant FR 21-860**